Absolute measurements of neutron yields from DD and DT implosions at the OMEGA laser facility using CR-39 track detectors

J. A. Frenje,[a] C. K. Li, F. H. Séguin, D. G. Hicks,[b] S. Kurebayashi, and R. D. Petrasso[c]
Plasma Science and Fusion Center, Massachusetts Institute of Technology, Cambridge, Massachusetts 02139

S. Roberts, V. Yu. Glebov, D. D. Meyerhofer, T. C. Sangster, J. M. Soures, C. Stoeckl, and C. Chiritescu
Laboratory for Laser Energetics, University of Rochester, New York, 14623

G. J. Schmid and R. A. Lerche
Lawrence Livermore National Laboratory, Livermore, California 94550

(Received 17 December 2001; accepted for publication 25 April 2002)

The response of CR-39 track detectors to neutrons has been characterized and used to measure neutron yields from implosions of DD- and DT-filled targets at the OMEGA laser facility [T. R. Boehly *et al.*, Opt. Commun. **133**, 495 (1997)], and the scaling of neutron fluence with R (the target-to-detector distance) has been used to characterize the fluence of backscattered neutrons in the target chamber. A Monte-Carlo code was developed to predict the CR-39 efficiency for detecting DD neutrons, and it agrees well with the measurements. Neutron detection efficiencies of $(1.1 \pm 0.2)\times 10^{-4}$ and $(6.0\pm 0.7)\times 10^{-5}$ for the DD and DT cases, respectively, were determined for standard CR-39 etch conditions. In OMEGA experiments with both DD and DT targets, the neutron fluence was observed to decrease as R^{-2} up to about 45 cm; at larger distances, a significant backscattered neutron component was seen. The measured backscattered component appears to be spatially uniform, and agrees with predictions of a neutron-transport code. As an additional application of the calibration results, it is shown that the neutron-induced signal in CR-39 used in charged-particle spectrometers on OMEGA can be used to determine DD and DT yields ranging from about 10^{10} up to 10^{14}. With further improvements in the processing and analysis of CR-39, this upper limit can be increased by at least two orders of magnitude. © *2002 American Institute of Physics.* [DOI: 10.1063/1.1487889]

I. INTRODUCTION

Implosions of targets filled with deuterium (D_2) or a mixture of deuterium and tritium (DT) gas are routinely performed at the OMEGA laser facility,[1] with neutron yields ranging from 10^6 up to 10^{14}. Neutrons are produced in the targets through the primary fusion reactions

$$D+D\rightarrow {}^3He(0.8\ \text{MeV})+n(2.45\ \text{MeV}) \quad (1)$$

and

$$D+T\rightarrow \alpha(3.6\ \text{MeV})+n(14.1\ \text{MeV}), \quad (2)$$

and measurements of the yields provide information about the quality of the implosions. Various diagnostics exist for detecting these neutrons and inferring different implosion parameters, and details about these techniques can be found in Refs. 2–5. In this article, we describe a new method of measuring neutron yields with CR-39 track detectors.[6] This approach makes possible the use of many small detectors simultaneously, for measuring neutron fluence as a function of position in a target chamber (useful for studying yields and backscatter from the target chamber, and for benchmarking neutron transport codes). The characterization of CR-39 response to neutrons is interesting in its own right, and it also provides information that helps clarify the performance of CR-39 in other applications (such as charged-particle spectrometry)[7–11] when neutrons are present. The neutron-response calibrations described here expand greatly on earlier work[12–14] and extend the applicability to situations relevant to inertial-confinement-fusion contexts.

The principles of the CR-39 response to charged particles and neutrons, and processing and analysis of CR-39, are discussed in Sec. II along with a description of Monte-Carlo simulations. In Sec. III, measurements of DD and DT neutrons at OMEGA are used to characterize the CR-39 response, and the DD results are shown to agree with Monte-Carlo predictions. These results are then used to measure neutron fluences as a function of angle and distance to the target, as described in Sec. IV. We finally discuss, in Sec. V, the relevance of this study to charged-particle measurements performed at OMEGA using CR-39. In this section, we also describe how the charged-particle measurements can be improved.

[a]Electronic mail: frenje@psfc.mit.edu
[b]Present address; Lawrence Livermore National Laboratory, Livermore, California 94550.
[c]Also a visiting Senior Scientist at the Laboratory for Laser Energetics, University of Rochester, New York 14623.

II. DETECTION OF NEUTRONS WITH CR-39

The detection of a neutron with CR-39 occurs in two steps. The first is the generation of a moving charged particle, either through scattering or through a nuclear reaction, as described below in Sec. II B. The second is detection of the track of the charged particle. We therefore begin with a discussion of the detection of charged particles.

A. Charged-particle interactions with CR-39

CR-39 is a clear plastic whose chemical composition is $C_{12}H_{18}O_7$. When a charged particle passes through, it leaves a trail of damage along its track in the form of broken molecular chains and free radicals. The amount of local damage along the track is related to the local rate at which energy is lost by the particle (dE/dx, where x is distance along the track). Particle tracks are made visible by etching the CR-39 in sodium hydroxide (NaOH). The surface of the plastic is etched at a rate called the bulk etch rate (V_B), while damaged material along particle tracks etches at a higher rate. The etch results in a conical pit wherever a particle passed through the plastic surface. With increased etch time, the diameter and depth of the pit increases as long as the depth remains smaller than the particle range in CR-39. These pits, or ''tracks,'' can be identified and quantified by the study of microscope images as described in Sec. II C.

In comparison with other track materials, CR-39 is more sensitive to low-energy (~MeV) protons. CR-39 is also relatively insensitive to electrons, x-rays and gamma rays, which is not the case for some other materials such as nuclear emulsions. These features of CR-39 make it the preferred detector choice for neutron measurements in high-flux fusion environments.

B. Neutron interactions with CR-39

Possible interactions of DD neutrons (2.45 MeV) and DT neutrons (14.1 MeV) with CR-39 are illustrated in Fig. 1. Either type of neutron can scatter elastically, producing recoil protons or carbon or oxygen nuclei in the forward direction in the laboratory system.[15] DT neutrons can also undergo inelastic (n,p) or (n,α) reactions with carbon or oxygen, and the resulting charged particles can produce tracks on the front and/or the back side of the CR-39. The neutron detection efficiency of CR-39 is the probability that an incident neutron results in a charged particle leaving a visible track on the surface of the CR-39 after etching.

For the elastic-scattering process, detection efficiency for neutrons incident on the front side of the CR-39 depends on the range r of recoil ions in the CR-39, and the etch depth l_e [which is equal to the bulk-etch rate $V_B(\approx 2.0\ \mu\text{m/h})$ times the etch time t]. For neutrons traveling approximately normal to the CR-39 surface, the front-side detection efficiency should be proportional to l_e if $l_e < r$, and independent of l_e if $l_e > r$. This is a consequence of the forward scattering and the fact that the number of potential scattering targets seen by neutrons is proportional to l_e. Tracks will also appear on the back side of the CR-39, where the detection efficiency is nearly independent of l_e and the initial CR-39 thickness $l_{\text{CR-39}}$ as long as $l_e \leqslant l_{\text{CR-39}} - r$. Nearly all detected tracks will be due to protons, because scattered carbon and oxygen ions have short ranges in CR-39. These processes will be clarified further in Sec. II D. In Sec. III we will discuss the results of experimental measurements and Monte-Carlo simulations of detection efficiencies.

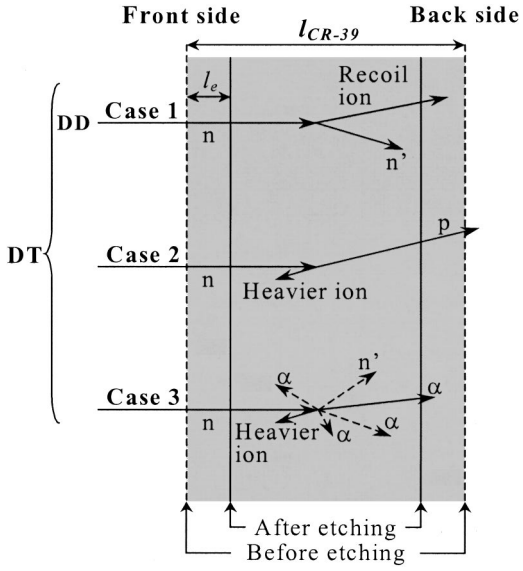

FIG. 1. Schematic drawing (not to scale) of the CR-39 track detector and the interaction processes taking place in the CR-39 material. The DD and DT neutrons can interact with the CR-39 material via elastic scattering, producing recoil protons or carbon or oxygen nuclei in the forward direction in the laboratory system (case 1). The DT neutrons can also inelastically react [via (n,p) and (n,α) reactions in carbon or oxygen] in the CR-39 material producing charged particles that can produce tracks on the front and/or the back side of the CR-39. Case 2 shows the (n,p) reaction, while case 3 shows both (n,α) reaction (solid arrows) and the carbon breakup reaction (dashed arrows) producing three α particles. Also indicated in the figure are initial CR-39 thickness $l_{\text{CR-39}}$, and CR-39 front and backside surfaces before and after etching, which results in an etch depth l_e.

C. Processing and analysis of CR-39

The diameters of tracks after etching depend mainly on the etch time (t) and the etch rate (V_B), where the latter is sensitive to the normality and the temperature of the NaOH. In order to get repeatable results, these factors must be controlled. In the work described here, the CR-39 samples were etched in 6.0 molarity NaOH held at 80 °C (all results will correspond to these conditions unless noted otherwise). An additional control on consistency is incorporated by exposing a small area on the backside of each piece of CR-39 to 5.5-MeV alphas (from a 0.1-μCi ^{241}Am source). With similar etch conditions these alphas should always give rise to tracks of the same size, but if this is not the case (due to variations in either etch conditions or CR-39 characteristics) corrections can be made to the other measured diameters by appropriate scaling.

After the etch process, CR-39 is inspected using an optical microscope with transmission lighting and infrared blocking filters. A computer-based scan system is necessary to characterize the thousands of tracks that are typically incident on large scan areas. A CCD camera captures images of the CR-39 for track analysis, and each track event is characterized by several parameters in order to differentiate the

signal from the intrinsic noise.[16] A manual focusing technique is applied in order to maintain the optimal focus to within a few microns, allowing for accurate characterization of the tracks.

The uncertainty in the determination of track diameter is mainly due to the finite pixel size and to focusing variations, and is a fraction of a micron. The tracks appear as dark circles on a light background. The perimeter of each track, which defines the area of the track, is identified as the location at which the image intensity drops below a specified ''boundary threshold,'' which is typically set to 85% of the median background intensity. The diameter is calculated from the area of the track. In addition, parameters such as optical contrast and track eccentricity are recorded. The optical contrast is calculated as the deviation (in percent) from background brightness. The contrast is important partly because it helps differentiate real tracks (which tend to be dark) from intrinsic-noise tracks in the CR-39 (which are often lighter in appearance). A contrast threshold of 65% will normally result in the acceptance of all neutron-induced tracks and at the same time the rejection of most intrinsic-noise tracks. The eccentricity of the track is determined from the shape of the track boundary relative to perfect circularity. In the case of CR-39 response to neutrons, a large fraction of the tracks are noncircular due to the angles of recoil particles and the reaction products. An eccentricity threshold of 35% is therefore used in this study for accepting all neutron-induced tracks, while 15% is more typical when analyzing tracks produced by charged particles with normal incidence. All results presented in this article are determined using analysis thresholds of (border/contrast/eccentricity)=(85/65/35), except as noted in Fig. 12.

D. Simulating CR-39 response to neutrons

A Monte-Carlo code was developed to calculate the absolute CR-39 response to DD neutrons, and to calculate the *np*-elastic scattering component for DT neutrons. The input parameters are the CR-39 area, the CR-39-to-target distance (R), and the neutron energy; the thickness $l_{\text{CR-39}}$ of the CR-39 is assumed fixed at 1050 μm. Using these input parameters, the efficiency is calculated for detecting a neutron by finding a track of a recoil proton on the front side or the backside of the CR-39.

For the calculation of front-side response, the *np*-scattering points are uniformly distributed in the etched CR-39 volume (region A in Fig. 2). For the backside calculation, scattering points are distributed in the whole CR-39 volume excluding the etched volume on the backside (regions A and B of Fig. 2). Attenuation of the neutron flux and multiple scattering effects in the CR-39 volume are ignored (attenuation of the neutron flux is at worst 10^{-3}, for $l_{\text{CR-39}}=1050$ μm, and the probability of multiple scattering is smaller). The target is assumed to be a point source of neutrons, and the *np*-scattering points in the CR-39 relative to the target determine the directions of incoming neutrons. The directions of the recoil protons are randomly generated, with the angular dependence of the *np*-differential elastic scattering cross section (in the laboratory system) as a weighting

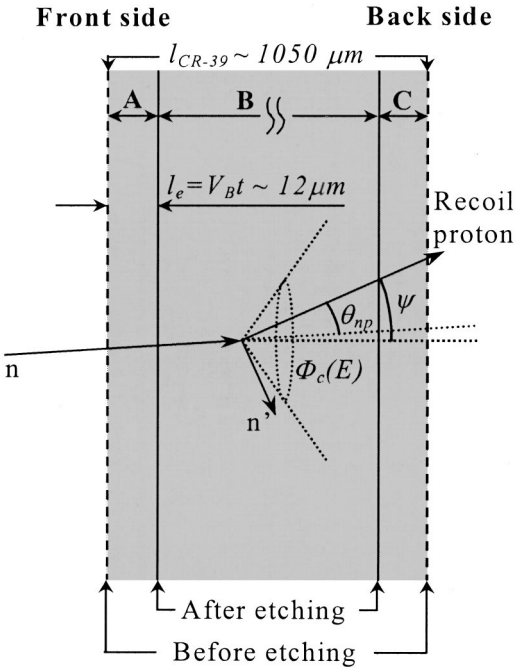

FIG. 2. Schematic drawing (not to scale) showing the *np*-elastic scattering process and the parameters used in the calculations of the neutron detection efficiencies on the front side (left) and the back side (right) of a CR-39 track detector. The input parameters are the CR-39 area, the detector-to-target distance (R), and neutron energy; the thickness $l_{\text{CR-39}}$ of the CR-39 is assumed fixed at 1050 μm. Using these input parameters, the efficiency is calculated for detecting a neutron by finding a track of a recoil proton on the front side or the backside of the CR-39 after etching. Elastic *np*-scattering points are uniformly distributed in the etched CR-39 volume for the front-side calculation (region A, characterized by the etch depth $l_e = V_B t \sim 12$ μm for a 6 h etch), and in the whole CR-39 volume excluding the etched volume for the backside calculation (regions A and B, characterized by the length $l_{\text{CR-39}} - l_e$). The recoil proton is assumed detected if the energy is within the CR-39 sensitivity range 0.2–6 MeV, and if the recoil angle (ψ), relative to the surface normal, is less than the critical angle ($\phi_c(E_p)$). ψ is equal to θ_{np} for incident neutrons traveling perpendicular to the CR-39 surface.

function (Fig. 3), and the scattering angle (θ_{np}) of the recoil proton relative to the incoming neutron determines the initial energy of the proton. The distance traveled by a proton between the *np*-scattering point and the (postetch) CR-39 surface is calculated, and the energy loss function (dE/dx) for the protons in plastic determines the proton energy at the surface. The recoil proton is assumed detected if the energy is within the CR-39 sensitivity range 0.2–6 MeV, and if the recoil angle (ψ), relative to the surface normal, is less than the critical angle $\phi_c(E_p)$.[19,20] Figure 4 shows the critical angle and the proton-recoil scattering angles (for both the DD and the DT case) as a function of initial proton energy. It can be seen in the figure that practically all recoil protons are detected for the DD case, while most are rejected based on scattering angle for the DT case. The total number of recoil particles (per incoming neutron) satisfying these requirements determines the CR-39 track detection efficiency. This procedure applies for both front and back side calculations.

The hydrogen number density in CR-39 (5×10^{22} cm^{-3}), the total *np* elastic-scattering cross section (0.7 b for 14 MeV neutrons and 2.5 b for 2.45 MeV neutrons), and the thickness of the source volume producing recoil protons determine the absolute detection efficiency

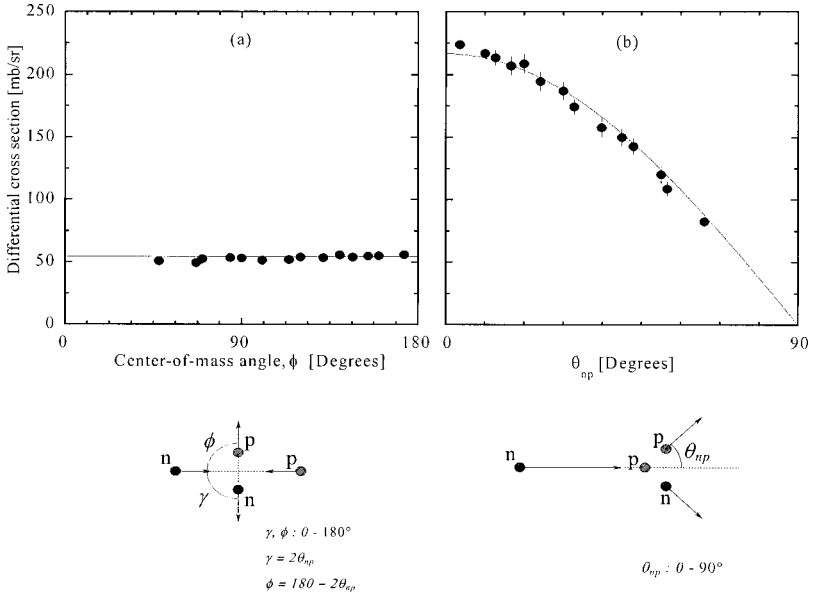

FIG. 3. (a) Differential *np*-elastic cross section given in the center-of-mass system for DT neutrons. The data were taken from Refs. 17 and 18, and the solid line is the best horizontal fit to the data. (b) Differential *np*-elastic cross section as a function of laboratory angle for the DT neutrons. It can be seen that the cross section peaks at forward-scattering angles in the laboratory system. The differential cross section in the laboratory system, shown in (b), was used in the calculations presented here, and is related to the center-of-mass cross section by $[d\sigma(\theta_{np})/d\Omega)]_{\rm lab}=4\cos\theta_{np}[d\sigma(\phi)/d\Omega)]_{\rm CM}$. Here, the scattering angle in the center-of-mass system, ϕ, is related to the scattering angle in the laboratory system, θ_{np}, by $\phi=\pi-2\theta_{np}$. The scattering process, in the two different observation systems, is schematically shown below the corresponding data. The DD-differential cross section looks nearly the same except that the total cross section is about 3.5 times larger.

(the uncertainties in these parameters are of the order of a percent). Simulations were performed for a variety of scenarios assuming a bulk-etch rate (V_B) of (2.0 ± 1.0) μm/h,[11] and the results are presented in Sec. III. The uncertainty in V_B is the dominant error in the simulations.

III. MEASURED AND SIMULATED CR-39 RESPONSE TO NEUTRONS

A. CR-39 efficiency for detecting DD neutrons

Following the discussion in Sec. II B, CR-39 efficiency for detecting DD neutrons on the front side should vary linearly with etch time; on the backside it should be independent of etch time. These features were experimentally verified in experiments at OMEGA. Four stacked CR-39 track detectors, with aluminum filters (thickness$>$100 μm) in between, were used at a location 15 cm from a D_2-filled target [see Fig. 5(a)]. Each CR-39 piece was then etched for 3, 4, 5, and 6 h; Fig. 6(a) shows the results and a comparison with data simulated as described in Sec. III D. The experimental data points are normalized to the neutron yield 1.34×10^{11} (shot 19556) measured by the indium-activation diagnostic located 25 cm from the target.[21] It can be seen that the experimental results agree well with the simulations over the 3–6 h range. An efficiency of $(1.1\pm0.2)\times10^{-4}$ was deter-

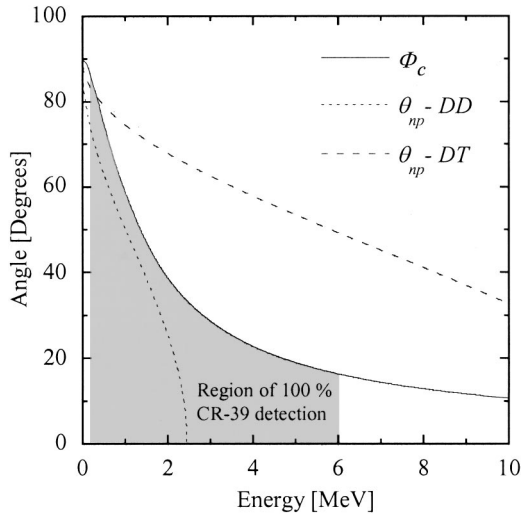

FIG. 4. Critical angle $[\phi_c(E_p)]$ and proton-recoil scattering angles (θ_{np}) for the DD and the DT case as functions of proton energy $(E_p=E_n\cos^2\theta_{np}^2)$. It is assumed that the neutrons have perpendicular angle of incidence, i.e., $(\psi=\theta_{np}$, see Fig. 2). As a result, practically all recoil protons for the DD case are detected, while most recoil protons for the DT case are rejected on the basis of scattering angle.

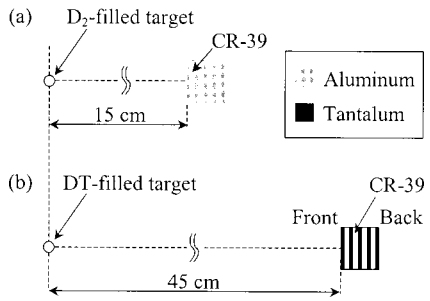

FIG. 5. Schematic drawing (not to scale) of the experimental setup of the CR-39 track detectors in OMEGA target chamber for the DD-neutron measurements [results presented in Fig. 6(a)] (a), and for the DT-neutron measurements [results presented in Fig. 6(b)] (b). In the DD case, four CR-39 track detectors were separated by aluminum filters, each at least 100 μm thick. The CR-39-aluminum assembly was located 15 cm from the target. In the DT case, five CR-39 track detectors were located 45 cm from the target where each piece of CR-39 was separated by a filter made of tantalum (thick enough to stop reaction products from an adjacent CR-39 track detector). The experimental setup, in both cases, allowed for several front and backsides of the CR-39.

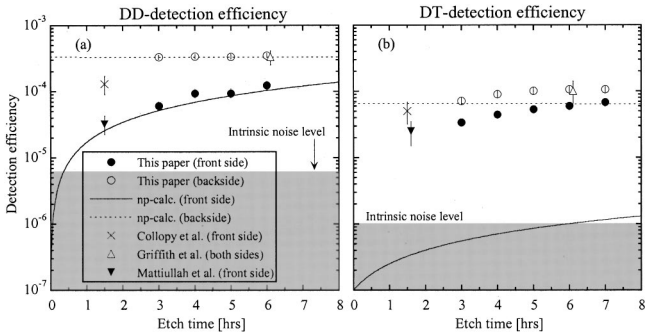

FIG. 6. Measured and calculated efficiencies for detecting DD (a) and DT neutrons (b), on the front and back sides of the CR-39 as a function of etch time. It can be seen that the DD simulations agree with the experimental results. The DT calculation includes only the elastic *np*-scattering component, which on the front side is dominated by the inelastic contributions (case 2 and 3 in Fig. 1). The experimental data are normalized to the neutron yields measured by indium and copper activation for the DD shot 19556 ($Y_n = 1.34\times 10^{11}$), and the DT shot 20228 ($Y_n = 6.7\times 10^{12}$), respectively. The CR-39 pieces were etched from 3 to 7 h. A nominal value of 300 intrinsic-noise tracks per cm^2 is used to calculate the corresponding detection efficiency limit at 15 and 45 cm for the DD and DT cases, respectively.

mined for detecting DD neutrons on the front side (with a 6 h etch), while $(3.3\pm 0.3)\times 10^{-4}$ was found for the backside. The quoted error bar (here and for all DD data in the article) is due to a combination of counting statistics and intrinsic noise.

The results reported in this study are in qualitative agreement with measurements performed by Mattiullah *et al.*[12] and by Griffith *et al.* (who quote an efficiency of about 3.3×10^{-4} for detecting neutrons in the energy range 1.5–6.0 MeV, including the response on both sides of the CR-39)[13] as indicated in Fig. 6(a). Our results appear to be a factor of four lower than the efficiency reported by Collopy *et al.*,[14] who found a CR-39 efficiency of $(1.3\pm 0.4)\times 10^{-4}$ for 2.9 MeV neutrons on the front side (for a 2 h etch of the CR-39 in NaOH held at 70 °C and 6.25 molarity). A possible explanation of the high detection-efficiency value reported by Collopy *et al.* is that a significant number of backscattered neutrons may have been detected. In addition, objects near the CR-39 (polyamide or other CR-30) may have generated extra charged particles that were detected within the CR-39 under test. In any event, care should be exercised when comparing the results from different studies because it is necessary to take into account different neutron energies, different etch techniques, different scanning methods, and differences in CR-39 properties.

B. CR-39 efficiency for detecting DT neutrons

For the case of DT neutrons, the situation is more complicated. In addition to elastic *np*-scattering, inelastic processes occur and must be accounted for. No Monte-Carlo calculations were performed to predict the absolute CR-39 efficiency for detecting DT neutrons (only the elastic *np* component was calculated). Instead, a measurement with a copper-activation diagnostic located 45 cm from the target was used for absolute calibration.[22] In these experiments, five pieces of CR-39, with tantalum filters in between, thick enough to stop reaction products from an adjacent CR-39 track detector, were located at 45 cm from a target that produced 6.7×10^{12} DT neutrons (shot 20218). Tantalum was selected as filter material for the DT case, instead of aluminum, because it has negligible (n,p) and (n,α) reaction cross sections at the DT neutron energy. This feature of tantalum minimizes the effect of external charged-particle sources that would artificially enhance the apparent CR-39 detection efficiency for DT neutrons (further information about filter selections for different applications is found in Sec. V). The experimental arrangement is schematically shown in Fig. 5(b). Each CR-39 piece was etched for 3, 4, 5, 6, and 7 h, and the results are presented in Fig. 6(b) as a function of etch time. It can be seen that in contrast to the DD case, the backside detection efficiency increases with etch time (up to about 6 h). This is a strong indication of (n,p) and (n,α) reactions in carbon and oxygen, in region C of Fig. 2, producing protons and heavier ions that are emitted in the backward directions. Some of the tracks detected on the backside are also caused by forward-scattered protons (produced in regions A and B of Fig. 2) generating a detection-efficiency component which is quite insensitive to the etch time [see the efficiency curve, in Fig. 6(a), for detecting DD neutrons on the backside]. The saturation of the backside detection efficiency at about 6 h also suggests that heavier ions, such as alphas and beryllium ions, are produced in the backward direction with average energies of about 3 and 6 MeV, respectively [further etching makes $l_e > r$ for these particles in CR-39]. Other heavier ions are produced as well, but their contributions to the detection efficiency are negligible in comparison.

Efficiencies of $(6.0\pm 0.7)\times 10^{-5}$ and $(1.0\pm 0.2)\times 10^{-4}$ were measured for detecting DT neutrons on the front and back sides of the CR-39, respectively (6 h etch). Tracks detected on the front side are caused mainly by alphas and heavier ions coming from (n,p) and (n,α) reactions in carbon and oxygen in region B, since most of the protons scattered in region A are excluded on the basis of critical angle (see Fig. 3). The quoted error bars for the DT case include track counting statistics in addition to a 10% systematic error introduced by the uncertainty in the copper activation measurement of the DT yield.

As shown in Fig. 6(b), these results are basically compatible with results reported by Mattiullah *et al.*[12] and by Griffith *et al.*[13] (who quote an efficiency of 1.3×10^{-4} for detecting neutrons in the energy range 6–18 MeV on both sides of the CR-39). Collopy *et al.*[14] determined an efficiency of $(5.0\pm 1.8)\times 10^{-5}$ (2 h etch in 6.25 molarity NaOH held at 70 °C) for detecting 14.8 MeV neutrons on the front side of the CR-39, which is somewhat higher than would be extrapolated from our data. Once again, it should be pointed out that only a qualitative comparison can be made due to the different neutron energies, different etch techniques, different scanning methods, and differences in CR-39.

C. Studies of track-diameter distributions

Additional information about CR-39 response to DD and DT neutrons can be acquired from the track diameter distributions shown in Fig. 7. A study of CR-39 response to dif-

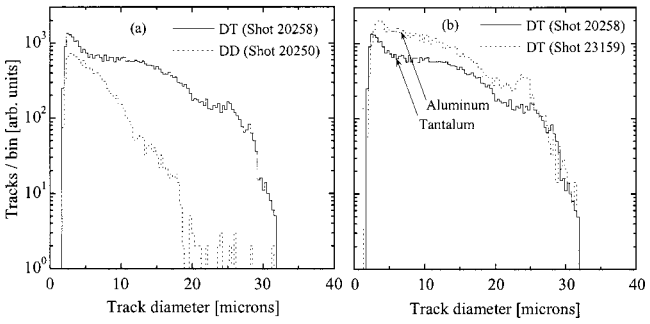

FIG. 7. (a) Distribution of tracks produced by DD and DT neutrons on the front side of the CR-39 for shot 20250 ($Y_n = 9.17 \times 10^{10}$ DD neutrons) and ofshot 20258 ($Y_n = 8.34 \times 10^{12}$ DT neutrons), respectively. The CR-39 track detectors were located at 15 and 45 cm from the target for the DD and DT cases, respectively. In the DD case, most tracks are smaller than 20 μm in diameter, which is an indication that mainly protons are produced. In the DT case, on the other hand, tracks larger than 20 μm in diameter are observed, indicating that nuclear reactions take place in the CR-39. (b) Track-diameter distributions resulting when aluminum (dashed line) and tantalum (solid line) filters are used in front of the CR-39, located at 60 and 45 cm from the target, respectively. The distributions were recorded during two different shots. To compare these distributions, the aluminum case was normalized to the tantalum case on the basis of the neutron yields, the distances to the target, and backscatter effects.

ferent charged particles (described in Ref. 10) showed that protons produce tracks up to about 20 μm in diameter (6 h etch). This can be seen for the DD case [Fig. 7(a)] where only recoil protons are detected (the contributions from recoil carbon and oxygen ions are negligible). For the DT case, on the other hand, tracks larger than 20 μm in diameter are observed [Figs. 7(a) and 7(b)], indicating that heavier ions are produced[11] from (n,p) and (n,α)-reactions.

In CR-39-based, charged-particle measurements made during OMEGA experiments (see Sec. V),[7–11] aluminum filters are used to slow particles down to energies where they are efficiently detected. For the DT case, aluminum also acts as a source of protons and heavier ions [produced in (n,p) and (n,α) reactions] which result in tracks that appear as noise in the data. This feature of aluminum could compromise the charged-particle studies, especially when charged-particle yields are low. This is illustrated in Fig. 7(b), where CR-39 track-diameter distributions recorded behind aluminum and tantalum filters are compared; the aluminum results in about 60% more tracks in the diameter range 2–25 μm.

IV. MEASUREMENTS OF NEUTRON FLUENCES AS A FUNCTION OF POSITION IN THE OMEGA TARGET CHAMBER

Determination of absolute CR-39 neutron-detection efficiencies has made possible absolute measurement of neutron fluences as a function of position in the OMEGA target chamber. In addition to quantifying neutron yields from imploded targets, these measurements provide information about angular and radial fluence variations. In Sec. IV A it is shown that there are negligible angular variations; in Sec. IV B it is shown that the radial variation differs from R^{-2} for $R \geqslant 60$ cm (where R is distance from target to detector), indicating the presence of neutron backscatter within the target chamber.

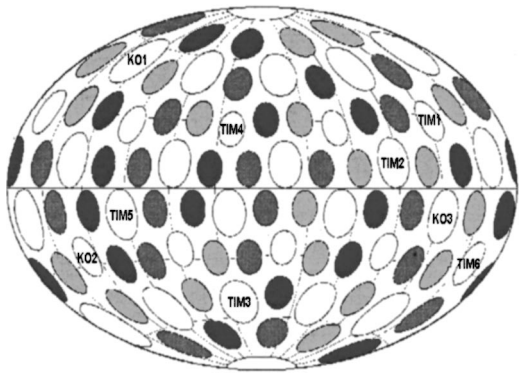

FIG. 8. OMEGA port diagram, showing the locations of TIM 1 through TIM 6, and KO 1 through KO 3, which were used for the CR-39 track detectors.

A. Angular uniformity

Figure 8 shows the arrangement of diagnostic ports on the OMEGA target chamber. CR-39 track detectors were positioned at a number of different ports, but all at the same R, for each shot in a series of experiments. Neutron yields were extracted from the back sides of the CR-39 pieces, and are plotted in Figs. 9 and 10 as a function of CR-39 location. In the DD case (Fig. 9), the detectors were positioned at 15 cm from the target; the measurements are on average in agreement with the In-activation-implied yield, which is also shown in the figure. A small variation is observed within the set of CR-39 measurements, but they are consistent with counting statistics and the effects of intrinsic noise. The conclusion is that there is no evidence of angular variations in the neutron fluence.

DT data were acquired in four different shots, using a different target-detector distance for each shot. As shown in Fig. 10, the results indicate both negligible angular variation and close agreement with activation-measured yields (in this

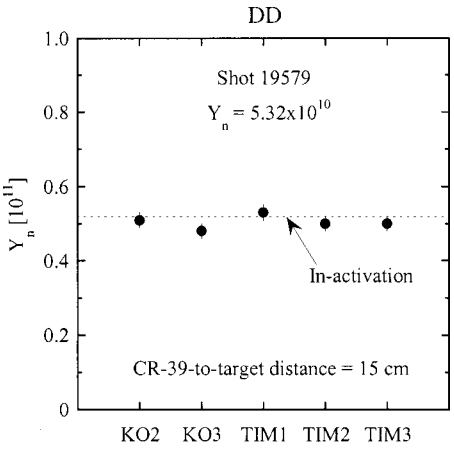

FIG. 9. Derived DD-neutron yields (Y_n) as functions of the CR-39 angular location for one shot (see Fig. 8 for the port positions). The CR-39 were all located 15 cm from the target. The neutron yields are extracted from the back sides of the CR-39, and the measurements are on average in agreement with the In-activation-implied yield (shown as the dashed line). A small variation is observed within the set of CR-39 measurements, but they are consistent with counting statistics and the effects of intrinsic noise. As a result, the CR-39 data suggest that the neutron fluence is independent of the angle at this distance.

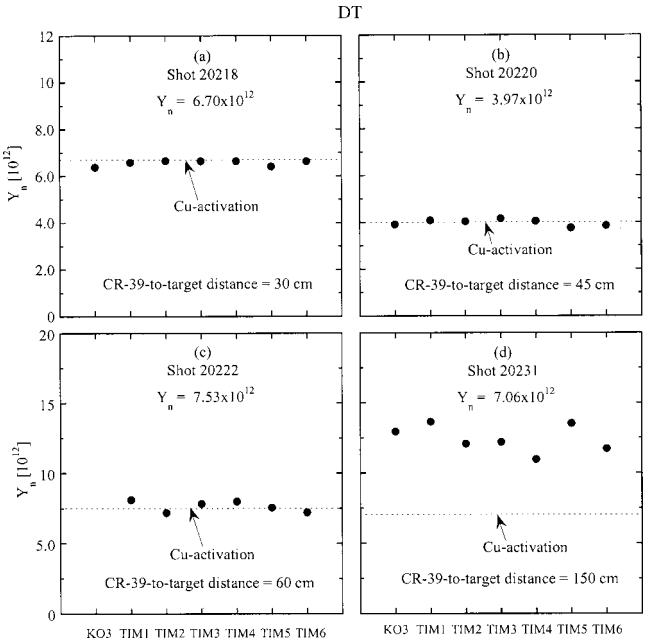

FIG. 10. Derived DT neutron yields (Y_n) as functions of the CR-39 angular location for four different shots, using a different target-detector distance for each shot. The results show both negligible angular variation and close agreement with Cu-activation-measured yields for distances up to about 60 cm from the target (a)–(c). (d) At 150 cm, the CR-39-measured yields are about a factor of 2 higher than the Cu-activation-measured yield, and this increased must be assigned to neutrons scattered from the target chamber wall. A variation of the neutron fluence of 15% about the mean is also seen at 150 cm, and this might be explained by neutron scattering from internal structures of the OMEGA target chamber.

case copper activation).[22] At 150 cm, the CR-39-measured yields are about a factor of 2 higher than the activation-measured yield, and we will see in Sec. IV B that this is due to neutrons scattered from the chamber wall. A variation of the neutron fluence by 15% about the mean is also seen at 150 cm, and this might be explained by neutron scattering from internal structures of the OMEGA target chamber (although this seems to be inconsistent with a conclusion reached in Sec. IV B based on backscatter simulations).

B. Radial variations

Having demonstrated that angular yield variations are not significant, it is possible to study radial variations by placing different detectors at different ports and at values of R varying from 15 to 150 cm (the inner radius of the target chamber is 156.2 cm). The number of neutron-induced tracks per cm^2 on the backsides of the detectors are plotted as a function of R for a DD shot and a DT shot in Fig. 11. Also shown in the figure are predictions of the radial variations in fluence that would be expected in the absence of backscatter, based on the activation-measured neutron yields for each shot and the CR-39 neutron-detection efficiencies found in Sec. III.

For the DD case [Fig. 11(a)] the experimental data do not significantly deviate from the R^{-2} predictions for distances up to the maximum of $R=60$ cm at which data were acquired. The intrinsic-noise level[23] (indicated in the figure) makes measurements at larger R uncertain and prevents any

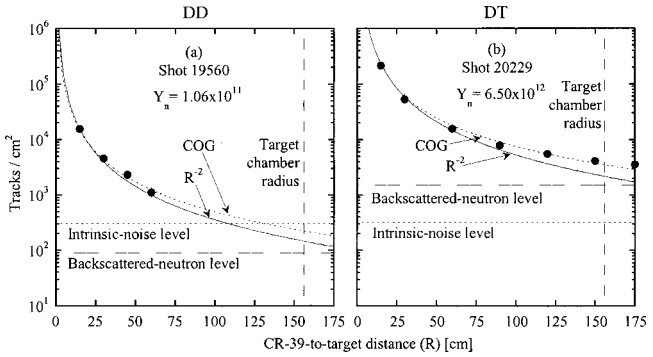

FIG. 11. Number of neutron induced tracks per cm^2 as a function of CR-39-to-target distance (R) for the DD case (a) and the DT case (b). The number tracks were measured on the backsides of the CR-39, after an intrinsic noise level of 300 tracks per cm^2 was subtracted (horizontal dotted lines). The solid lines indicate the R^{-2} predictions, which are based on the determined detection efficiencies and the neutron yields (Y_n) specified in the figures. The neutron-transport calculations, using the code COG, are shown as dotted line. The experimental data and the calculations indicate a significant component of backscattered neutrons from the target chamber, which has an inner radius of 156.2 cm (indicated as the vertical dashed lines), for $R \geqslant 60$ cm. The COG calculation also indicates, in comparison with the R^{-2} prediction, that the backscattered neutron emission is quite uniform (as shown by the horizontal dashed line) in the target chamber for both the DD case and DT case.

direct experimental conclusion about the level of backscattered neutrons. However, the neutron transport code COG[24] was used to predict the backscattered neutron component for distances up to 175 cm.[25] The results, shown in Fig. 11(a) in terms of detectable tracks in CR-39, indicate that the backscattered neutron component is quite uniform in the target chamber and contributes a number of tracks (about 90 per cm^2) that is below the intrinsic-noise level by about a factor of 3. This means that the backscatter component cannot be studied with CR-39 unless the neutron yield becomes high enough for the backscatter-induced track density to exceed the intrinsic-noise level. As we will see, this is exactly what happens for DT data.

Figure 11(b) shows the experimental data and COG predictions for a DT shot. Because of the high neutron yield, the intrinsic-noise level is significantly lower than both the measured track densities and the predicted backscatter component. This makes measurements significant even at $R=175$ cm, and allows us to see that there are definite deviations from the R^{-2} prediction for $R \geqslant 60$ cm. These deviations are consistent with the COG predictions, confirming the presence of a backscattered neutron component and suggesting that it is spatially uniform.

V. CHARACTERIZATION OF NEUTRON-INDUCED NOISE IN CHARGED-PARTICLE MEASUREMENTS AT OMEGA USING CR-39 TRACK DETECTORS

CR-39 is used in a wide variety of charged-particle spectrometry measurements during experiments at OMEGA.[7–11] The characterization of CR-39 response to DD and DT neutrons, discussed in Secs. II–IV, provides a better understanding of the neutron-induced noise in the charged-particle measurements. It also suggests that the neutron-induced noise can be reduced for DT implosions by careful choice of

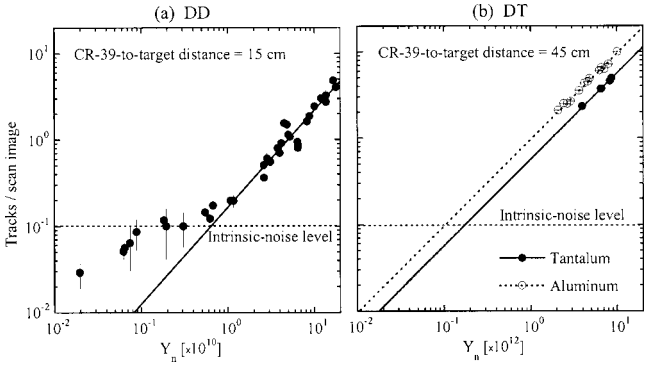

FIG. 12. (a) Number of DD-neutron-induced tracks (within the diameter range 6–12 μm) per scan image (1.3×10^{-3}cm^2) as a function of implosion yield (where the yield was measured with either indium activation or a neutron time-of-flight diagnostic). The data were extracted from the front sides of the CR-39 using scan parameters (85/65/15). The CR-39 detectors were located 15 cm from the target in all cases. The solid line indicates a linear fit to the data above a neutron yield of 10^{10}, indicating that useful yield estimates can be made in that regime. Intrinsic noise, nominally indicated by the horizontal dotted line, dominates at lower yields. (b) Number of DT-neutron-induced tracks (within the diameter range 6–12 μm) per scan image is plotted as a function of DT neutron yield determined from copper activation. The data were acquired using aluminum or tantalum filters in front of the CR-39. The CR-39 pieces were located 45–60 cm from the targets, but all data are normalized to 45 cm by correcting for R^{-2} and for backscatter effects. It can be seen that the aluminum filter acts as an external charged-particle source and increases the number of neutron-induced tracks by about 60% in the CR-39 (relative to tantalum). The DT data show a strong linear correlation between track density and neutron yield, and extrapolation to lower neutron yield indicates that at 15 cm from the target the method should work down to at least 10^{10}, where intrinsic noise would start to dominate. There is an upper limit on yield for this method of about 10^{14}, where track overlap in the CR-39 starts to be significant.

filter materials (the filter material is not important for DD implosions because the DD neutron energy is below the reaction thresholds for most materials). In addition, the ability to calculate a neutron yield from the same piece of CR-39 used for charged-particle measurements can be useful for verifying the consistency of the recorded target-detector distance and the neutron yields reported by other diagnostics. The neutron yield can be studied on most pieces of CR-39 used in charged-particle spectrometers as long as the number of neutron-induced tracks exceeds the number of intrinsic-noise tracks, because there is usually a ''no-signal'' area of the CR-39 surface that is not exposed to the charged particles from the target.

We now look at data from D_2-filled capsules and DT-filled capsules, and we restrict our attention to CR-39 tracks in the diameter range 6–12 μm (6 h etch) because for many applications this is the range actually used for analysis.[11]

A. Studies of DD implosions

For DD studies at OMEGA, no-signal regions in the charged-particle data were used and the results are plotted in Fig. 12(a). This figure shows the number of tracks per unit area as a function of implosion yield (where the yield was measured with either indium activation or a neutron time-of-flight diagnostic). The CR-39 detectors were located 15 cm from the target in all cases. The data show a strong linear correlation between track density and neutron yield as long as the yield exceeds 10^{10}, indicating that useful yield estimates can be made in that regime. Intrinsic noise dominates at lower yields.

B. Studies of DT implosions

For DT implosions, the neutron energy is above the reaction thresholds for most materials. This indicates that care must be exercised when selecting a filter material, and from the results of Sec. III C, it can be predicted that tantalum would result in fewer neutron-induced events than the aluminum that is used in most current applications. Figure 12(b) illustrates actual data acquired with these two filter materials during OMEGA implosions. The number of tracks (within diameters range 6–12 μm) in no-signal areas is plotted as a function of DT neutron yield, as determined through copper activation. The detectors were located 45–60 cm from the targets, but all are normalized to 45 cm by correcting for R^{-2} and for backscatter effects as measured in Sec. IV B. It can be seen that the aluminum filter (data shown as open circles) acts as an external charged-particle source and increases the number of neutron-induced tracks by about 60% in the CR-39 (relative to tantalum data, which is shown as black-filled circles). Tantalum clearly has advantages over aluminum for noise minimization.

The data show a strong linear correlation between track density and neutron yield, indicating that yield estimates can be made from track densities. Extrapolation to lower neutron yield indicates that at 45 cm from the target the method should work down to at least 10^{11}, where intrinsic noise would start to dominate; at 15 cm from the target the yield limit would be 10^{10}. There is an upper limit on yield for this method of about 10^{14}, where track overlap in the CR-39 starts to be significant. With further improvements in processing and scanning of CR-39, and correction for track overlap,[26] the upper limit can be extended to yields around 10^{16} and perhaps as high as 10^{17} (the upper limit at the National Ignition Facility would be about ten times higher).

ACKNOWLEDGMENTS

The authors would like to express our appreciation to the OMEGA Laser and Experimental Operation and Target Fabrication crews for their excellent work and continuous support. This work has been supported in part by LLE (Subcontract No. P0410025G) and LLNL (Subcontract No. B313975), and by the U. S. Department of Energy Office of Inertial Confinement Fusion under Cooperative Agreement NO. DE-FC03-92SF19460, the University of Rochester, and New York State Energy Research and Development Authority. The support of DOE does not constitute an endorsement by DOE of the views expressed in this work.

[1] T. R. Boehly *et al.*, Opt. Commun. **133**, 495 (1997).
[2] M. D. Cable *et al.*, Rev. Sci. Instrum. **63**, 4823 (1992).
[3] O. Delage *et al.*, Rev. Sci. Instrum. **66**, 1205 (1995).
[4] R. A. Lerche *et al.*, Rev. Sci. Instrum. **66**, 933 (1995).
[5] R. J. Leeper *et al.*, Rev. Sci. Instrum. **68**, 868 (1997).
[6] The CR-39 track detectors used in these experiments were manufactured by Track Analysis Systems Limited, Bristol, U.K.
[7] C. K. Li *et al.*, Phys. Plasmas **7**, 2578 (2000).
[8] D. G. Hicks *et al.*, Phys. Plasmas **7**, 5106 (2000).

[9] F. H. Séguin *et al.*, Phys. Plasmas **9**, 2725 (2002).
[10] C. K. Li *et al.*, Phys. Plasmas **8**, 4902 (2001).
[11] F.H. Séguin *et al.*, Rev. Sci. Instrum. (submitted).
[12] Mattiullah *et al.*, Nucl. Instrum. Methods Phys. Res. B **51**, 76 (1990).
[13] Griffith *et al.*, Lawrence Livermore National Laboratory, UCRL-82657 (1980).
[14] M. T. Collopy *et al.*, Rev. Sci. Instrum. **63**, 4892 (1992).
[15] Neutron-Cross Sections, Vol. 2, National Nuclear Data Center, Brookhaven National Laboratory.
[16] The intrinsic noise is mainly due to structural defects in the CR-39, or debris on the surface of the CR-39 that look similar to real particle track.
[17] J. C. Allred *et al.*, National Nuclear Data Center, Brookhaven National Laboratory.
[18] J. D. Seagrave *et al.*, National Nuclear Data Center, Brookhaven National Laboratory.
[19] Particles with recoil angles, relative to the surface normal, larger than the critical angle $[\phi_c(E_p)]$ are not detected. The critical angle depends on the particle type, properties of the track-detector, and the etch conditions.
[20] P. M. Stafford *et al.*, Nucl. Tracks Radiat. Meas. **14**, 373 (1988).
[21] The (n,n')-reaction in indium, which has a reaction threshold of 0.5 MeV, is used for measurement of the DD neutron yield. The effect of the backscattered neutrons is negligible at the short target-to-detector distance.
[22] The $(n,2n)$ reaction in copper, which has a reaction threshold of 10.9 MeV, is used for measurement of the DT neutron yield. As for the indium activation diagnostic, the effect of the backscattered neutrons is negligible at the short target-to-detector distance.
[23] A nominal value of 300 intrinsic-noise tracks per cm^2 is normally used in the analysis. However, this number, which varies from CR-39 to CR-39 piece, is strongly dependent on the analysis procedure used.
[24] R. M. Buck and J. M. Hall, Proc. SPIE **3771**, 127 (1999).
[25] The OMEGA target chamber was modeled as a 9-cm-thick, spherical aluminum shell. A more complicated model of the OMEGA target chamber, using exact shape and dimensions, and including internal structures in the target chamber, did not yield an appreciably different result. This reinforces the view that the backscattered neutrons are coming primarily from the target chamber wall.
[26] The track overlap limitation can be extended to considerably higher track densities using statistical analysis techniques that correct for the track overlap.